INFECTION AND IMMUNITY, Mar. 2004, p. 1265–1274 Vol. 72, No. 3
0019-9567/04/$08.00+0 DOI: 10.1128/IAI.72.3.1265–1274.2004

A 38-Kilobase Pathogenicity Island Specific for *Mycobacterium avium* subsp. *paratuberculosis* Encodes Cell Surface Proteins Expressed in the Host

Janin Stratmann,[1]† Birgit Strommenger,[1]† Ralph Goethe,[1] Karen Dohmann,[1] Gerald-F. Gerlach,[1]* Karen Stevenson,[2] Ling-ling Li,[3] Qing Zhang,[3] Vivek Kapur,[3] and Tim J. Bull[4]

Institute for Microbiology, Department of Infectious Diseases, School of Veterinary Medicine, Hannover, Germany[1]; Moredun Research Institute, International Research Centre, Penicuik, Scotland,[2] and Department of Surgery, St. George's Hospital Medical School, London,[4] United Kingdom; and Department of Microbiology and Biomedical Genomics Center, University of Minnesota, Minneapolis, Minnesota[3]

Received 12 June 2003/Returned for modification 4 September 2003/Accepted 13 November 2003

We have used representational difference analysis to identify a novel *Mycobacterium avium* subsp. *paratuberculosis*-specific ABC transporter operon (*mpt*), which comprises six open reading frames designated *mptA* to *-F* and is immediately preceded by two putative Fur boxes. Functional genomics revealed that the *mpt* operon is flanked on one end by a *fep* cluster encoding proteins involved in the uptake of Fe^{3+} and on the other end by a *sid* cluster encoding non-ribosome-dependent heterocyclic siderophore synthases. Together these genes form a 38-kb *M. avium* subsp. *paratuberculosis*-specific locus flanked by an insertion sequence similar to IS*1110*. Expression studies using Western blot analyses showed that MptC is present in the envelope fraction of *M. avium* subsp. *paratuberculosis*. The MptD protein was shown to be surface exposed, using a specific phage (fMptD) isolated from a phage-peptide library, by differential screening of *Mycobacterium smegmatis* transformants. The phage fMptD-derived peptide could be used in a peptide-mediated capture PCR with milk from infected dairy herds, thereby showing surface-exposed expression of the MptD protein in the host. Together, these data suggest that the 38-kb locus constitutes an *M. avium* subsp. *paratuberculosis* pathogenicity island.

Paratuberculosis, also called Johne's disease, is a severe and incurable enteritis of ruminants caused by *Mycobacterium avium* subsp. *paratuberculosis* and has a considerable economic impact on the livestock industry (21, 28). In cattle, infection most commonly occurs in newborn calves by the fecal-oral route. However, clinical symptoms, predominantly including persistent diarrhea and weight loss, are usually delayed in animals until 3 to 5 years of age (13). Paratuberculosis is prevalent in domestic animals and many species of wildlife worldwide, including primates (31). In addition, *M. avium* subsp. *paratuberculosis* has been isolated from intestinal tissue of Crohn's disease patients, and its potential role as a zoonotic pathogen is currently being investigated (12, 22).

Previous attempts to determine the molecular cause for pathogenicity of *M. avium* subsp. *paratuberculosis* have focused on the identification of antigenic proteins (16, 26) and the characterization of secreted components by using monoclonal antibodies (32). Further studies have identified an *M. avium* subsp. *paratuberculosis*-specific low-GC cassette carrying genes with putative functions related to lipopolysaccharide or extracellular polysaccharide biosynthesis (47) and have identified cross-reactive, species- and subspecies-specific epitopes (32). In addition, an *M. avium* subsp. *paratuberculosis*-specific ferric reductase which is secreted in vivo and in vitro has been described (25). Other potential virulence factors reported include a serine protease (10) and a fibronectin attachment protein (41). However, closely related homologues of these factors can be found in *M. avium* subsp. *avium* and *Mycobacterium tuberculosis*, and they are unlikely to be *M. avium* subsp. *paratuberculosis* specific.

In this study we have investigated the hypothesis that, as has been shown in other bacterial species, unique membrane proteins and secretory pathways are likely to be critical features involved in *M. avium* subsp. *paratuberculosis* pathogenicity (7, 17, 18, 20). We have used representational difference analysis (RDA) (30, 45, 47) to identify a 7-kb *M. avium* subsp. *paratuberculosis*-specific ABC transporter operon (*mpt*). Proteins from this operon were shown to contain putative membrane-spanning regions and to be expressed on the mycobacterial cell surface in vitro and in vivo. We further show that this ABC transporter operon is preceded by two putative Fur boxes and represents part of an *M. avium* subsp. *paratuberculosis*-specific 38-kb putative pathogenicity island that includes several iron uptake-related gene clusters.

MATERIALS AND METHODS

Bacterial strains, plasmids, primers, and growth conditions. The bacterial strains, plasmids, and primers used in this study are listed in Table 1. Mycobacteria were grown on Middlebrook 7H10 agar or in Middlebrook 7H9 medium (both from Difco Laboratories, Detroit, Mich.) supplemented with oleic acid-albumin-dextrose-catalase enrichment (Difco), Tween 80 (0.05%), and kanamycin (40 μg ml^{-1}) for *Mycobacterium smegmatis* transformants; for *M. avium* subsp. *paratuberculosis* culture, mycobactin (2 μg ml^{-1}) (Synbiotics, Lyon, France) was added. *Escherichia coli* strains were grown in Luria-Bertani medium supplemented with appropriate antibiotics (ampicillin, 100 μg ml^{-1}; kanamycin, 40 μg ml^{-1}).

* Corresponding author. Mailing address: Tierärztliche Hochschule Hannover, Zentrum für Infektionsmedizin Institut für Mikrobiologie, Bischofsholer Damm 15, D-30173 Hannover, Germany. Phone: 49 (511) 856-7598. Fax: 49 (511) 856-7697. E-mail: gfgerlach@gmx.de.

† J.S. and B.S. contributed equally to this work.

TABLE 1. Characteristics of strains, phages, plasmids, and primers used in this study

Strain, phage, plasmid, primer, peptide	Characteristics, reference, and/or source[a]
Strains	
M. avium subsp. *paratuberculosis* strain 6783	Clinical isolate, DSM 44135
14 *M. avium* subsp. *paratuberculosis* bovine clinical isolates	Fecal and lymph node isolates from clinically diseased cattle from different herds in northern Germany
M. avium subsp. *avium* strain ATCC 25291	DSM 44156
M. smegmatis mc^2155	42
M. scrofulaceum	NCTC 10803
M. bovis BCG	NCTC 5692
M. bovis	NCTC 10772
M. kansasii	NCTC 10268
M. microti	NCTC 8710
M. gordonae	NCTC 10267
M. fortuitum	NCTC 10394
E. coli DH5αF′	F′/*endA1 hsdR17* ($r_K^- m_K^+$) *supE44 thi-1 recA1 gyrA* (Nal^r) *relA1* Δ(*lacZYA-argF*) *U169 deoR* [ϕ80d*lac*Δ(*lacZ*)*M15*] (35)
Phage fMptD	Phage isolated from the Ph.D.-12 phage display library with the specific sequence 5′-GGG AAG AAT CAT CAT CAG CAT CAT AGG CCT CAG-3′
Plasmids	
pUC19	*E. coli* cloning vector carrying an ampicillin resistance determinant (Pharmacia)
pGEX5x-3	*E. coli* expression vector for the construction of glutathione *S*-transferase fusion proteins (Pharmacia)
pMV361	Integrative mycobacterial shuttle vector carrying a kanamycin resistance determinant (9)
pRDIII300	Fragment RDIII300 in pUC19 (this work)
pRDIII301	Fragment RDIII301 in pUC19 (this work)
pRDIII302	4-kb *Dpn*II fragment in pGH432 obtained by hybridization with a probe derived from the 5′ end of RDIII300 (this work)
pRDIII303	4-kb *Dpn*II fragment in pGH432 obtained by hybridization with a probe derived from the 3′ end of RDIII300 (this work)
pRDIII320	Fragment RDIII300 in pMV361 (Fig. 1, inset) (this work)
pRDIII320Δ1	Deletion derivative of pRDIII320 with a 3,201-bp *Fse*I fragment deleted (Fig. 1, inset) (this work)
pRDIII320Δ2	Deletion derivative of pRDIII320 with a 2,410-bp *Sma*I-*Sac*I fragment deleted (Fig. 1, inset) (this work)
pRDIII350	PCR fragment obtained with primers ABC3 and ABC4, cut with *Bam*HI and *Eco*RI, and ligated into pGEX5x-3
Primers	
RBam12	5′-GAT CCT CGG TGA-3′ (29)
RBam24	5′-AGC ACT CTC CAG CCT CTC ACC GAG-3′ (29)
IPIII30	5′-CTA TGC GCA CTG ACG CTT C-3′ (this work)
IPIII31	5′-TTC CGA AGA ATC CGA TGA G-3′ (this work)
ABC3	5′-CCG C**GG ATC C**GC TTA CGA CGG AGG TCA A-3′ (this work)
ABC4	5′-GCC **GGA ATT C**GA TGT TGA TGA GAAT CCC T-3′ (this work)
ISMav1	5′-GTA TCA GGC CGT GAT GGC GG-3′
ISMav2	5′-CGC CAC CAG CGC TCG ATA CA-3′
Peptides	
aMptD	Biotin-aminohexacarbonic acid-GKNHHHQHHRPQ
aMPr	Biotin-aminohexacarbonic acid-HSQPKQVKKASR (control peptide)

[a] The nucleotides in boldface indicate the restriction enzyme sites used for cloning into pGEX5x-3. DSM and NCTC strains were from the Deutsche Gesellschaft für Mikroorgansismen und Zellkulturen (Braunschweig, Germany) and the National Collection of Type Cultures (Colindale, United Kingdom), respectively.

RDA and isolation of RDA fragments. Mycobacterial chromosomal DNA was extracted according to the method described by Bose and coworkers (6). A simplified RDA technique (45) using total genomic DNA digested with *Bcl*I was used to subtract the driver strain genome of *M. avium* subsp. *avium* ATCC 25291 from the test strain genome of *M. avium* subsp. *paratuberculosis* isolate 6783 (DSM 44135). An *M. avium* subsp. *paratuberculosis*-specific *Bcl*I fragment was identified and designated RDIII30; it was further used to identify larger fragments by Southern blot analyses of *M. avium* subsp. *paratuberculosis* DNA digested with *Kpn*I and *Sac*I. Hybridizing fragments were cloned and designated RDIII300 (*Kpn*I fragment) and RDIII301 (*Sac*I fragment). Based on the sequence information for RDIII300 and RDIII301, a third and a fourth overlapping fragment, designated RDIII302 and RDIII303, were isolated from an *M. avium* subsp. *paratuberculosis* genomic library generated by a partial *Dpn*II digestion and ligation of fragments of 2 to 4 kb into pGH432 and pGH433 (Advanced Vectors Inc., Hopkins, Minn.). The specificity of the RDA fragment was confirmed by PCR with RDIII30-derived primers IPIII30 and IPIII31, using 14 bovine clinical *M. avium* subsp. *paratuberculosis* isolates and the reference strains of six other mycobacterial species (Table 1).

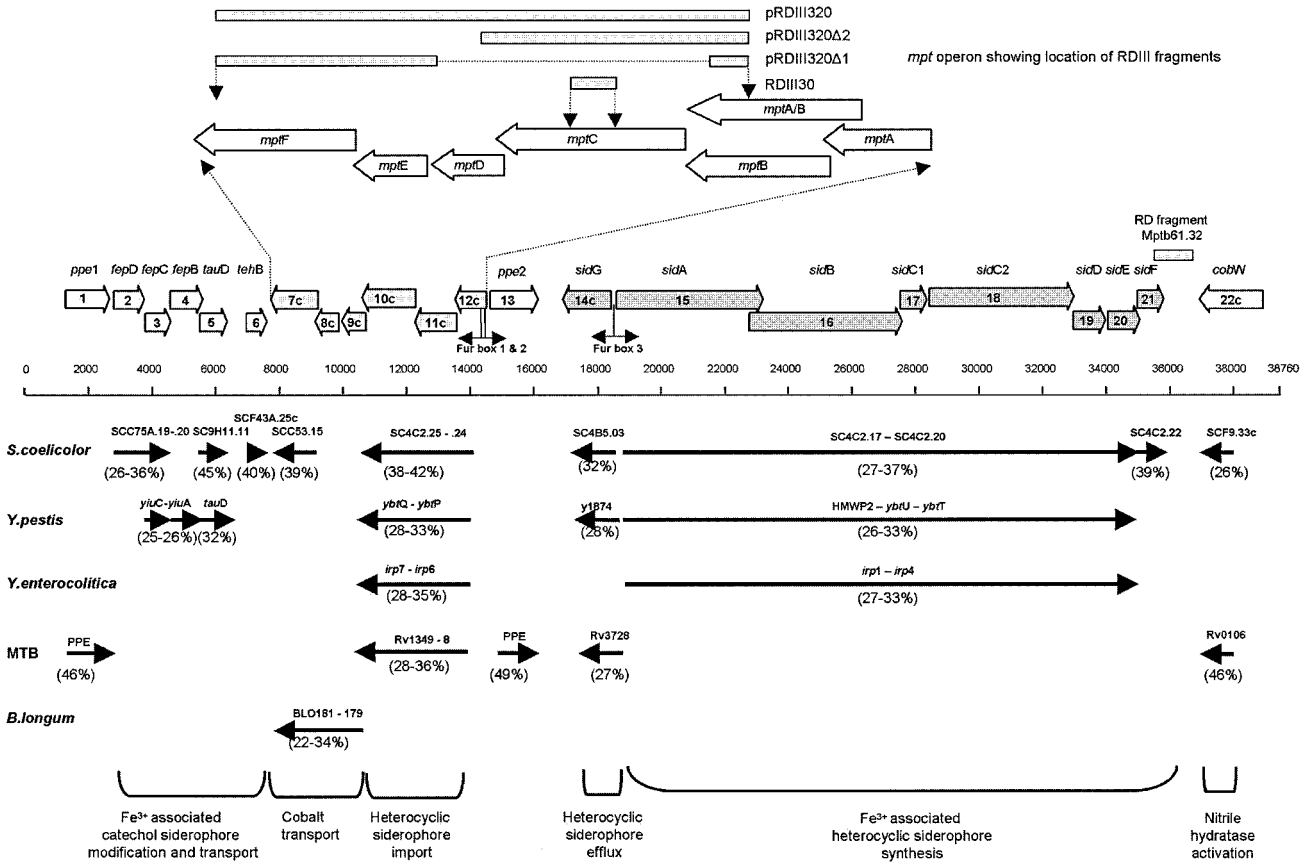

FIG. 1. Representation of ORFs and putative Fur boxes from the *M. avium* subsp. *paratuberculosis* 38-kb locus and identity of homologues in other bacteria. The inset shows the relative locations of the *mpt* ORFs with respect to the deletion derivatives constructed. Numbers in parentheses represent the percent identities of homologues to putative *M. avium* subsp. *paratuberculosis* ORFs.

Manipulation and analysis of DNA. Agarose gel electrophoresis, Southern blot analyses, plasmid preparation, PCR, DNA cloning, and transformation of *E. coli* were done by standard procedures (37). DNA-modifying enzymes were purchased from New England Biolabs (Karlsruhe, Germany). DNA sequencing was done by primer walking; primers were purchased from Invitrogen (Groningen, The Netherlands), and sequencing reactions were done by SeqLab (Göttingen, Germany). Sequencing data analyses were performed with the HUSAR 5.0 program (DKFZ, Heidelberg, Germany). Preliminary sequence data were obtained from the Institute for Genomic Research website at http://www.tigr.org. BLASTN and BLASTP engines were used through the National Center for Biotechnology Information portal (http://www.ncbi.nlm.nih.gov/BLAST). The *M. avium* subsp. *paratuberculosis* genome was searched by using Contig16, available from the University of Minnesota portal (http://www.ccgb.umn.edu/cgi-bin/common/web_blast.cgi).

Construction of recombinant mycobacterial shuttle plasmids and deletion derivatives and transformation in *M. smegmatis* mc²155. The 5,367-bp *Sac*I fragment RDIII300 (Fig. 1), containing the complete *mptC*, *mptD*, and *mptE* open reading frames (ORFs) and truncated *mptB* and *mptF* ORFs, was cloned into the mycobacterial shuttle vector pMV361 (Table 1) under control of the vector-based *hsp60* promoter. Based on this plasmid, designated pRDIII320, deletion derivatives were generated. Deletion of a 3,201-bp *Fse*I fragment resulted in plasmid pRDIII320Δ1 (Fig. 1), containing *mptE* and a partial *mptF* gene. Deletion of the DNA downstream of an *Sma*I restriction site by using a double digestion with *Sma*I and *Hpa*I resulted in plasmid pRDIII320Δ2 (Fig. 1), containing an intact *mptC* ORF. These plasmids were used to transform *M. smegmatis* mc²155 by electroporation as described previously (38).

Protein preparations, electrophoresis, and Western blotting. Mycobacterial whole-cell lysates were prepared from 100 mg of bacterial pellet harvested from Middlebrook liquid medium. Bacteria were resuspended in 500 μl of distilled water, and cell disruption was achieved by mechanical treatment for 190 s with zirconium beads in a mini-bead beater (Bio-Spec Products, Inc., Bartlesville, Okla.) followed by sonication. Residual cellular debris was removed by centrifugation (2,500 × *g*) for 10 min; total crude mycobacterial cell envelopes were obtained by ultracentrifugation (175,000 × *g*) for 2 h at 4°C and dissolved in 500 μl of Tris-EDTA buffer. Protein aggregates were prepared as previously described (19), and all protein preparations were analyzed by sodium dodecyl sulfate-polyacrylamide gel electrophoresis and Western blotting as described earlier (19). For the detection of the MptC protein in *M. avium* subsp. *paratuberculosis*, the ECL Western blotting detection system (Amersham Pharmacia Biotech, Freiburg, Germany) was used according to the manufacturer's instructions; for other Western blots, an alkaline phosphatase-labeled goat anti-rabbit conjugate and a substrate containing nitroblue tetrazolium and 5-bromo-4-chloro-3-indolylphosphate were used.

Preparation of antiserum. A DNA fragment obtained by PCR with primers ABC3 and ABC4 (Table 1) was cut with *Bam*HI and *Eco*RI and cloned into pGEX5x-3, resulting in plasmid pRDIII350 (Table 1). Upon induction with isopropyl-thiogalactoside (IPTG) (1 mM final concentration), inclusion bodies were formed and purified as described previously (19). Serum was raised in rabbits by an initial intracutaneous injection and two subcutaneous booster injections 3 and 6 weeks later, each with 100 μg of recombinant fusion protein in a total volume of 300 μl containing 30% adjuvant (Emulsigen-Plus; MVP Inc.).

Isolation and labeling of phages recognizing surface-exposed epitopes of an Mpt protein. Biopanning was performed based on the Ph.D.-12 phage display library (New England Biolabs), containing random 12-mer peptides with a complexity of 1.9×10^9. Phages were panned by using whole cells or cell envelopes coupled to cyanogen bromide-activated Sepharose of *M. smegmatis* transformants carrying pRDIII320. After amplification in *E. coli*, counterselection to remove nonspecific phages was done by absorption to whole cells or cell envelopes of *M. smegmatis* carrying the vector pMV361 only. This selective panning with counterselection was repeated five times with high-stringency washing con-

ditions in the last panning, as described previously (44). Both panning procedures resulted in the selection of the same phage, designated fMptD. Fluorescence labeling of phage particles was performed as previously described (44).

Enrichment of *M. avium* subsp. *paratuberculosis* from bulk milk. Peptide aMptD (GKNHHHQHHRPQ) was synthesized based on the sequence obtained from phage fMptD with amino-terminal biotinylation and amino-hexacarbonic acid as a spacer (Fa. Affina Immuntech, Berlin, Germany). The peptide was dissolved, coupled to paramagnetic particles (Promega Inc., Madison, Wis.), and used for peptide-mediated capture PCR on bulk milk from herds previously analyzed by this method with a different peptide (44). The specificity of the amplification product was confirmed by restriction enzyme digestion (data not shown).

RESULTS

RDA-based identification and cloning of an *M. avium* subsp. *paratuberculosis*-specific ABC transporter operon. An RDA approach comparing total genomic DNAs from *M. avium* subsp. *avium* and *M. avium* subsp. *paratuberculosis*, digested with *Bcl*I, identified a fragment of 340 bp designated RDIII30. The sequence of the RDIII30 fragment revealed one continuous ORF which encoded a putative transmembrane domain but showed no significant homology to GenBank sequences. Using the RDIII30 fragment as a probe, we identified and sequenced a further four overlapping fragments (designated RDIII300 to -303) by directed cloning of a *Sac*I fragment and a *Kpn*I fragment of the sizes predicted by Southern blot analyses (RDIII300 and RDIII301) and by screening a genomic library of *M. avium* subsp. *paratuberculosis* strain 6783 generated by the cloning of 2- to 4-kb fragments generated by a partial *Dpn*II digest (RDIII302 and RDIII303). This revealed an 8,745-bp contiguous sequence (accession number AF419325) which carried six putative ORFs (designated *mptA* to *mptF*) transcriptionally orientated in tandem. A BLASTN search of this sequence showed no significant homology to sequences from any of the bacterial genomes, including that of *M. avium* subsp. *avium*, currently in GenBank. The *M. avium* subsp. *paratuberculosis* specificity of the region was further supported by PCR with RDIII30-derived primers IPIII30 and IPIII31 and amplification a fragment of 247 bp from 14 bovine *M. avium* subsp. *paratuberculosis* isolates, with no product obtained from six other mycobacterial species (data not shown). Although PCR is not a foolproof method to demonstrate sequence specificity, as a polymorphism in the primer binding region can result in the absence of an amplification product, the combined outcome of the PCR and GenBank analyses is a strong indication for the *M. avium* subsp. *paratuberculosis* specificity of the sequence.

A genomic alignment of the completed *M. avium* subsp. *avium* (TIGR-104) genome and the recently completed *M. avium* subsp. *paratuberculosis* (K-10) genome revealed that the RDIII30 sequence is part of a 38-kb *M. avium* subsp. *paratuberculosis*-specific locus (GenBank accession number AE016958, located at coordinates 4146188 through 4184947 of the *M. avium* subsp. *paratuberculosis* K-10 genome) comprising 22 ORFs orientated into three major gene clusters, provisionally designated *fep*, *mpt*, and *sid* (Fig. 1). The locus is bounded on one side by an insertion element with 83% homology to IS*1110* (23) that is present as a single copy in *M. avium* subsp. *paratuberculosis* and in some strains of *M. avium* subsp. *avium* but not in the genome of the sequenced *M. avium* subsp. *avium* (TIGR-104) strain. The other side of the 38-kb locus contains sequence with 95% DNA homology over 23 kb to *M. avium* subsp. *avium* (TIGR-104), with the 38-kb locus starting from CGGCCCGGCGAG positioned in the *M. avium* genome at coordinate 5012818.

In this work the 38-kb locus was numbered for clarity as positions 1 to 38760 (the sequence with accession number AF419325 is located at position 6600 to 15344). A BLASTN search of the whole 38-kb locus sequence against GenBank confirmed the unique specificity of this region, which also includes the previously identified *M. avium* subsp. *paratuberculosis*-specific probe Mptb61.32 (43), located at positions 36208 to 36803 (Fig. 1).

Functional genomics of the *mpt* operon and the 38-kb locus. The lack of homology of the carboxy-terminal region of MptA to the GenBank protein database and the close homology of the amino-terminal region of MptA and carboxy-terminal region of MptB to the products of genes *rv1348* of *M. tuberculosis* and *sc4c2.24* of *Streptomyces coelicolor* (Table 2) suggest that both ORFs may combine to encode a single MptA-MptB protein. The ORFs of *mptA* and *mptB* overlap by 62 bp and contain a previously identified "slippery site" (CCC CCA at positions 13599 to 13604) (43) associated with programmed translational frameshifts. A similar frameshift resulting in the expression of a single transporter protein has been previously described for a permease protein belonging to an ABC transporter operon in *M. smegmatis* (2). We propose, therefore, that the putative start codon for MptA-MptB is at position 14040, encoding the carboxy-terminal region of ORF *mptA* only (Fig. 1) and, together with *mptB*, encoding an ORF of 589 amino acids in length. This start codon is supported by an associated Shine-Dalgarno consensus sequence (GAAGGA) and two putative transcriptional Fur box control motifs (38-kb locus positions 14079 to 14105 and 14504 to 14531) within putative bidirectional promoters upstream of this position. Both Fur boxes have significant homology (90 and 74%) (Fig. 2) to an *E. coli* Fur box consensus sequence (1), and Fur box 2 also has a perfect panlindromic structure.

The *mptA-mptB* ORF is immediately followed by two overlapping ORFs, *mptC* and *mptD*. The *mptC* sequence contains the RDA fragment RDIII30 and codes for a predicted protein of 593 amino acids in length with a calculated molecular mass of 64 kDa. Homology searches revealed significant degrees of identity to ABC transporter proteins from *S. coelicolor* (38%), *M. tuberculosis* (29%), and *Yersinia pestis* (28%). The putative MptC protein contains five predicted transmembrane domains, including Walker A and B motifs (5) and a Higgins motif (24) typical of ABC transporters and in positions identical to the homologues in *M. tuberculosis* and *Y. pestis* (data not shown).

Unlike other ORFs in the 38-kb region, *mptD* to *-F* do not have functional homologues in *Yersinia* spp. or *S. coelicolor*. Even though the *mptC* reading frame overlaps *mptD*, ORFs *mptD* to *-F* are more linked by their significant protein identities (22 to 34%) and similar genomic organization to a cobalt ABC transporter cassette found in the gut commensal *Bifidobacterium longum* (39). MptE contains a CbiQ functional motif (E value, $2E^{-13}$) and MptF contains a CbiO functional motif (E value, $3E^{-39}$), which are associated with active transport of cobalt into the cytosol. MptD has no predicted functional motifs, but TMHMM (algorithm for the prediction of transmembrane helices in proteins, accessible with the

TABLE 2. BLAST search results

ORF no.	ORF name (position in Fig. 1)	Length of ORF (amino acids)	Putative function	Homologue (species)	Identity (%)	Span (amino acids)	GenBank accession no.
1	*ppe1* (1070–2626)	518	PPE signaling membrane protein	Rv3018c (*M. tuberculosis*)	46	182	NP_217534
2	*fepD* (2684–3658)	324	FepD FeIII permease	SCC75A.19 (*S. coelicolor*)	26	324	CAB61719
3	*fepC* (3654–4464)	271	FepC FeIII ABC transporter with ATP binding domain	YiuC (*Y. enterocolitica*)	27	278	AAD29087
				SCC75A.20 (*S. coelicolor*)	36	224	CAB61720
4	*fepB* (4461–5498)	345	FepB FeIII ABC transporter	YiuA (*Y. pestis*)	25	356	NP_670175
5	*tauD* (5498–6274)	258	Taurine dehydrogenase	TauD (*Y. pestis*)	32	260	NP_671259
				Rv3406 (*M. tuberculosis*)	33	270	NP_217923.1
6	*tehB* (6885–7529)	214	TehB tellurite resistance protein, *S*-adenosyl-L-methionine dependent non-nucleic acid methyltransferase	SCF43A.25c (*S. coelicolor*)	40	193	NP_625135
7c	*mptF* (9162–7660)	500	ATP binding protein and CbiO ABC-cobalt transporter	BLO181 (*B. longum*)	34	486	ZP_00120392
				SCC53.15 (*S. coelicolor*)	39	215	NP_626571
8c	*mptE* (9851–9159)	230	CbiQ ABC-cobalt transporter	BLO180 (*B. longum*)	29	215	ZP_00120392
9c	*mptD* (9869–10495)	208	Unknown	BLO179 (*B. longum*)	22	194	ZP_00120391
10c	*mptC* (12273–10492)	593	ATP binding protein, putative ABC transporter	Rv1349 (*M. tuberculosis*)	29	583	NP_215865
				YbtQ (*Y. pestis*)	32	571	NP_405475
				Irp7 (*Y. enterocolitica*)	28	575	CAB46572
				SC4C2.25 (*S. coelicolor*)	38	585	NP_631729
11c	*mptB* (13628–12270)	452	ATP binding protein, putative ABC transporter	Rv1348 (*M. tuberculosis*)	36	573	NP_215864
				YbtP (*Y. pestis*)	38	421	NP_405474
				Irp6 (*Y. enterocolitica*)	34	508	CAB46573
				SC4C2.24 (*S. coelicolor*)	46	413	NP_631728
12c	*mptA* (14040–13567)	157	ATP binding protein, putative ABC transporter	Rv1348 (*M. tuberculosis*)	34	115	NP_215864
				SC4C2.24 (*S. coelicolor*)	37	126	NP_631728
13	*ppe2* (14702–16216)	504	PPE signaling membrane protein	Rv3018c (*M. tuberculosis*)	49	160	NP_217534
14c	*sidG* (18558–17026)	510	Metabolite efflux transporter	Y1874 (*Y. pestis*)	28	417	NP_669190
15	*sidA* (18728–23443)	1,571	Non-ribosome-dependent heterocyclic siderophore synthase	Irp2 (*Y. pestis*)	31	888	NP_405472
				HMWP2 (*Y. enterocolitica*)	31	891	P48633
16	*sidB* (23232–27896)	1,554	Non-ribosome-dependent heterocyclic siderophore synthase	Irp2 (*Y. pestis*)	27	980	NP_405472
				HMWP2 (*Y. enterocolitica*)	27	980	P48633
				SC4C2.17 (*S. coelicolor*)	32	737	NP_631721
17	*sidC1* (27893–28738)	281	Non-ribosome-dependent heterocyclic siderophore synthase	SC4C2.18 (*S. coelicolor*)	37	249	NP_631722
18	*sidC2* (28784–33391)	1,535	Non-ribosome-dependent heterocyclic siderophore synthase	Irp2 (*Y. pestis*)	29	1433	NP_405472
				HMWP2 (*Y. enterocolitica*)	29	1433	P48633

Continued on following page

TABLE 2—*Continued*

ORF no.	ORF name (position in Fig. 1)	Length of ORF (amino acids)	Putative function	Homologue (species)	Identity (%)	Span (amino acids)	GenBank accession no.
				SC4C2.17 (S. coelicolor)	34	1535	NP_631721
19	sidD (33388–34419)	343	Saccharopine dehydrogenase	SC4C2.19 (S. coelicolor)	27	354	NP_631723
20	sidE (34495–35529)	344	Oxidoreductase (NAD binding) heterocyclic siderophore synthase	SC4C2.20 (S. coelicolor)	30	352	NP_631724
				YbtU (Y. pestis)	32	242	T17441
				Irp3 (Y. enterocolitica)	32	242	T30343
21	sidF (35526–36278)	250	Thioesterase heterocyclic siderophore synthase	SC4C2.22 (S. coelicolor)	39	231	NP_631726
				YbtT (Y. pestis)	33	230	NP_405469
				Irp4 (Y. enterocolitica)	33	230	T30344
22c	cobW (38645–37425)	406	Nitrile hydratase	CobW (M. tuberculosis)	46	377	NP_214620

HUSAR 5.0 program [DKFZ, Heidelberg, Germany]) predictions indicate six transmembrane domains (data not shown), suggesting that MptD is a membrane-bound component in this system.

The *mpt* genes are positioned between the *sid* and *fep* clusters. The *sid* cluster is the largest of the putative operons and includes the genes *sidA* to *sidG* and possibly a gene encoding a membrane signaling protein (*ppe2*). These genes are contiguous but are orientated in groups transcribed in opposing directions enclosing a Fur box located at positions 18571 to 18597 (Fig. 2) between *sidG* and *sidA*. The ORFs *sidB* and *sidC1*, *sidC2* and *sidD*, and *sidE* and *sidF* are orientated in tandem with overlapping start and stop codons. Eleven of 12 predicted genes from these clusters have significant identities (24 to 42%) and are arranged in an organization similar to that of operons involved in the nonribosomal synthesis and membrane transport of Fe^{3+}-associated heterocyclic siderophore peptides from *Y. pestis* (3), *Yersinia enterocolitica* (11), and *S. coelicolor* (4). The *sid* cluster is followed by a putative nitrile hydratase homologue (*cobW*) at the end of the 38-kb island and is flanked by an IS*1110*-like insertion sequence. The *fep* cluster is a cluster of six ORFs, with four ORFs overlapping. The first ORF encodes a homologue (46% identity) of the *ppe* gene family in *M. tuberculosis* and is a probable membrane protein involved in signaling. Adjacent to this are three overlapping ORFs, *fepB* to *fepD* (Fig. 1), with significant identity (25 to 36%) and similar organization to genes in *Y. pestis* and *S. coelicolor* that are involved in the transport of catecholate Fe^{3+}-associated siderophore into the bacterial cytosol (40). Homologues of *fepC* and *fepD* are ABC transporters associated with the ability of catecholate siderophores to permeate through bacterial membranes. The putative FepC protein has an ATP binding motif signature (E value, $1E^{-38}$) suggesting that it is an active transport system. Homologues to FepB, such as YiuA of *Y. pestis*, are periplasmic substrate binding proteins associated with the transport of Fe^{3+} siderophores. The final two ORFs have significant functional motifs but have only minor connections with other *fep* systems. The first, *tauD*, overlapping *fepB*, has 32 to 37% identity to taurine deoxygenases of *S. coelicolor*, *Y. pestis*, and *Pseudomonas aeruginosa*. The second, *tehB*, contains a tellurite resistance motif (parse 6E-06) with significant homology to *S*-adenosyl-L-methionine-dependent non-nucleic acid methyltransferases of *S. coelicolor* (Table 2).

```
GATAATGATAATCATTTTC Consensus
........A....G..A.. M. paratuberculosis Fur-box 1 (14080-14099)
CG......A...G...... M. paratuberculosis Fur-box 2 (14506-14525)
..C.....A....G..... M. paratuberculosis Fur-box 3 (18572-18591)
A........T.......AT fepB E.coli         GenBank ECOFEPB
.........TT.....AA. tonB A.suis         GenBank AY101604
....T..G....T...A.. iroB S.enterica     GenBank YPU50452
......A.ATC......C. pchD P.aeruginosa   GenBank PAX82644
AT....A.....G.....G acn  L.pneumophila  GenBank LPNACNX
GTG...A....C....A.. ybtA Y.pestis       GenBank YPU50452
ACA.......GCA...A.. hutA V.cholerae     GenBank VIBHUTA
```

FIG. 2. Alignment of *M. avium* subsp. *paratuberculosis* 38-kb region putative Fur boxes with an *E. coli* consensus sequence and Fur boxes from several other pathogens. Dots indicate identical nucleotides, and numbers in parentheses indicate the base location.

Expression of Mpt proteins and their potential role in virulence. The predicted expression and localization of MptC and MptD in cell membranes were investigated by various methods. For MptC, Western blotting was performed with a serum raised in rabbits against a glutathione *S*-transferase–MptC fusion protein. No MptC protein was expressed by *E. coli* transformants (data not shown); however, a 64-kDa protein, consistent with the predicted size of MptC, could be demonstrated in envelope preparations of *M. avium* subsp. *paratuberculosis* and *M. smegmatis* transformed with MptC expression constructs, but not in controls (Fig. 3).

For MptD, a subtractive screening of an M13 phage peptide library was performed on envelope and whole-cell preparations of *M. smegmatis* transformed with the MptD expression construct pRDIII320, using *M. smegmatis* transformed with vector alone as a control. Both of these screens identified the same phage, designated fMptD, encoding the binding peptide designated aMptD (GKNHHHQHHRPQ). Fluorescein isothiocyanate (FITC)-labeled fMptD was used (Fig. 4A) to demonstrate specific binding of phage to the cell surface of *M. smegmatis* transformed with constructs expressing MptC-F (pRDIII320) but not with controls transformed with constructs expressing MptC (pRDIII320Δ2) or MptE-F (pRDIII320Δ1).

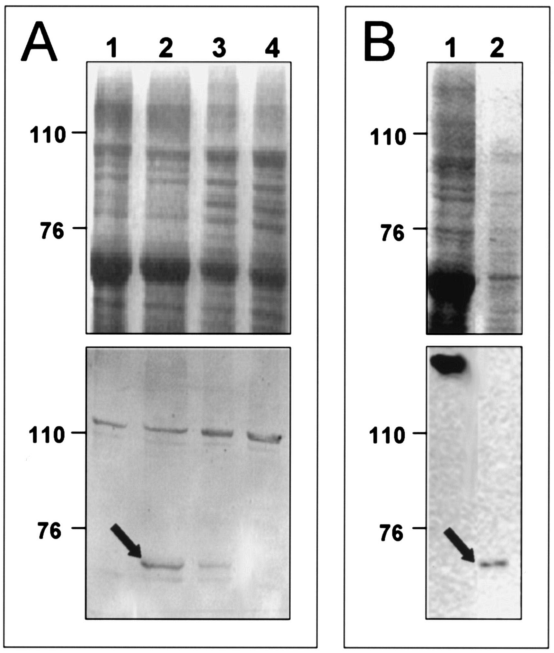

FIG. 3. Coomassie blue-stained gel (top) and Western blot (bottom) of crude membrane preparations. (A) Lanes 1 to 4, *M. smegmatis* mc^{2}155 transformants containing pMV361, pRDIII320, pRDIII320Δ2, and pRDIII320Δ1, respectively. (B) *M. smegmatis* (lane 1) and *M. avium* subsp. *paratuberculosis* (lane 2). The arrows indicate the position of the MptC protein detected by the serum raised against the recombinant fusion protein. The numbers on the left indicate the positions of protein markers in kilodaltons.

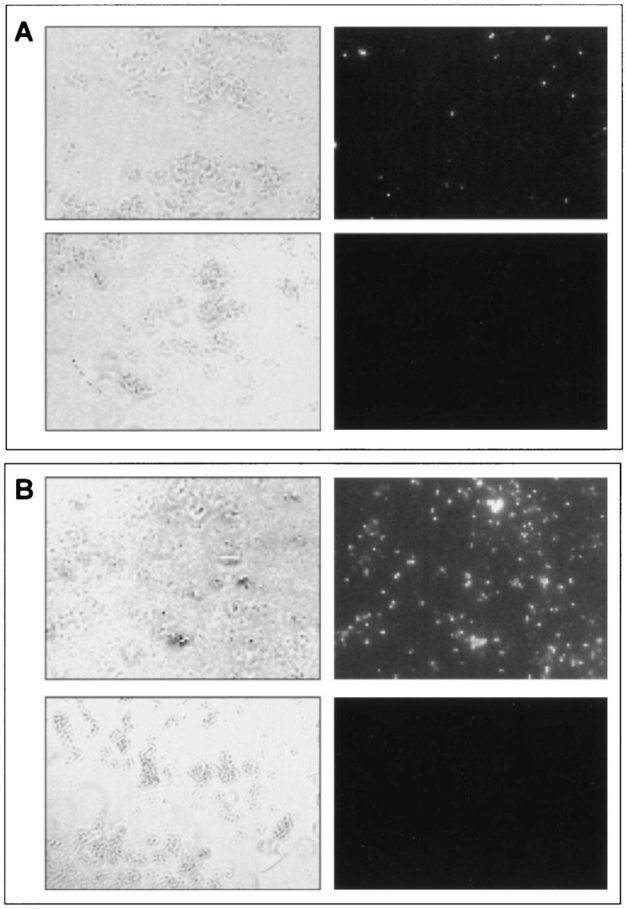

FIG. 4. Fluorescence microscopy with FITC-labeled phage fMptD as an affinity reagent. (A) *M. smegmatis* mc^{2}155 transformed with pRDIII320 (top panels) and pMV361 (bottom panels) observed by light microscopy (left panels) and immunofluorescence (right panels). (B) *M. avium* subsp. *paratuberculosis* (top panels) or *M. avium* subsp. *avium* (bottom panels) observed by light microscopy (left panels) and immunofluorescence (right panels).

In addition, FITC-labeled fMptD could detect *M. avium* subsp. *paratuberculosis*, but not *M. avium* subsp. *avium*, grown in Middlebrook 7H9 medium (Fig. 4B). These results strongly suggest that phage fMptD binds an epitope of a specific *M. avium* subsp. *paratuberculosis* protein, MptD, which is expressed and exposed on the cell surface.

To investigate the potential role of the *mpt* operon in *M. avium* subsp. *paratuberculosis* infection, peptide aMptD encoded by phage fMptD was synthesized and used in a peptide-mediated capture PCR to identify *M. avium* subsp. *paratuberculosis* within bulk milk samples from infected and noninfected dairy herds (Fig. 5). This result confirms the expression of cell surface-associated MptD protein by *M. avium* subsp. *paratuberculosis* during infection of the natural host.

DISCUSSION

In this work we have identified three novel *M. avium* subsp. *paratuberculosis* operons (*mpt*, *fep*, and *sid*) present within a 38-kb locus. The absence of significant DNA homology of the entire 38-kb region to *M. avium* subsp. *avium*, the presence of a previously described short sequence (Mptb61.32) that was also identified by RDA between *M. avium* subsp. avium and *M. avium* subsp. *paratuberculosis* (34), the positive PCR analyses with 14 clinical *M. avium* subsp. *paratuberculosis* isolates, and the negative PCR analyses with the reference strains of six other mycobacterial species strongly suggest that this locus is *M. avium* subsp. *paratuberculosis* specific. Functional genomic analysis revealed that most ORFs from the 38-kb locus have significant identities to previously identified proteins in other pathogens. Similarities in functional motifs which are consistent with an involvement in linked molecular processes primar-

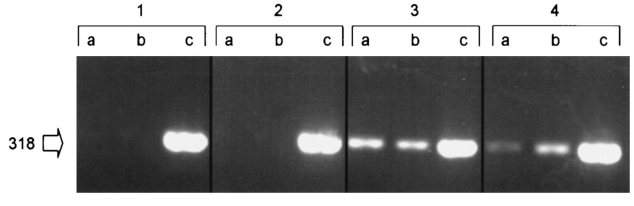

FIG. 5. Peptide aMptD-mediated capture PCR from *M. avium* subsp. *paratuberculosis*-negative (panels 1 and 2) and -positive (panels 3 and 4) bulk milk samples with IS*Mav2*-derived primers. Lanes a and b, products of PCRs of the sample; lanes c, internal positive control (sample spiked with *M. avium* subsp. *paratuberculosis* DNA). The arrow indicates the expected position of the PCR product in base pairs.

ily concerned with uptake of iron and other essential trace elements were also found. This is supported by the presence of Fe^{3+}-regulated transcriptional control motifs (Fur boxes) within putative promoters associated with the *sid* and *mpt* operons (11, 18), which are responsible for the translocation into the bacterial cytosol of Fe^{3+}, bound to a peptide siderophore. The putative MptE and -F proteins have homologues from the gut commensal *B. longum* (39) which contain motifs associated with active transport of cobalt into the cell cytosol. Identities to homologous proteins in other species are insufficient to suggest that cobalt is the ion involved in *M. avium* subsp. *paratuberculosis*, and many other ions, such as Fe^{3+} and Mn^{2+}, could be associated instead. However, the chelation of cobalt is important for intracellular survival and may be linked to *cobW*, located further down the 38-kb locus, as some nitrile hydratases require cobalt for activity (15). The role of the *mpt* operon in iron uptake is further supported, however, by the presence of two Fur boxes located immediately upstream of the *mpt* operon within a putative promoter region.

Homologues to proteins encoded by the *sid* operon are involved in the nonribosomal synthesis and membrane transport of Fe^{3+}-associated heterocyclic siderophore peptides from *Y. pestis* (3), *Y. enterocolitica* (11), and *S. coelicolor* (4). In these organisms, the operons are transcriptionally controlled by binding of proteins, such as the *furB* gene product, onto Fur box motifs positioned within associated promoters. *fur* genes have also been identified in several mycobacterial species; a role of *furA* in virulence has been postulated, as it modulates the response to oxidative stress by regulating the expression of the catalase:peroxidase. To date, nothing is known about the function of *furB*, which likewise is present in several mycobacterial species (36). The *sid* operon described in this work contains a 19-mer Fur box homologue with four mismatches to an *E. coli* consensus sequence (1) within a putative bidirectional promoter sequence. This suggests that the *sid* operon may have biosynthetic and transcriptional control mechanisms similar to the those of the *ybt* operon of *Yersinia* spp.

Homologues of proteins encoded by the *fep* operon (FepC and -D) in *Y. pestis* and *S. coelicolor* are ABC transporters associated with the ability of catecholate Fe^{3+} siderophores to permeate through bacterial membranes into the cytosol (40). The putative FepC protein has an ATP binding motif signature, suggesting that this is part of an active transport system. Homologues to the FepB protein, such as YiuA of *Y. pestis*, are periplasmic binding proteins also associated with the transport of Fe^{3+} siderophores. The TauD homologues are taurine deoxygenases which liberate sulfur from taurine for assimilation into processes such as cysteine biosynthesis (27) and may be crucial virulence determinants in intracellular persistence when access to sulfonated compounds is limited. The sequence divergence of the predicted *M. avium* subsp. *paratuberculosis* TauD protein suggests that it may have a different specific substrate that could possibly be a catechol siderophore. The putative TehB protein has significant homology to *S*-adenosyl-L-methionine-dependent non-nucleic acid methyltransferases whose function could be related to the catechol-*o*-methyltransferase activity on catechol siderophores observed with gene Rv1703c from *M. tuberculosis* (14).

The final ORF in the 38-kb locus, *cobW*, is located at the very end of the locus between the *sidA-F* cluster and IS*1110*. Its product contains a CobW motif and significant identity with Rv0106 of *M. tuberculosis* and with SCF9.33c of *S. coelicolor*. The function of this gene is uncertain, but the presence of a CobW motif suggests that it may be an activator of nitrile hydratase, an enzyme important in production of nitric oxide and whose biosynthesis is linked to Fe^{3+} regulation in macrophages (15).

We have investigated the expression and location of two proteins from the *mpt* operon, which support our in silico analyses. We have demonstrated the expression of MptC in *M. smegmatis* transformants, confirmed its predicted size, and shown it to be an envelope-associated protein. The expression of MptC in cell envelopes of *M. avium* subsp. *paratuberculosis* was also shown, supporting its putative function as an ABC transporter (18). In addition, an *M. avium* subsp. *paratuberculosis*-specific phage (fMptD) was isolated and used to demonstrate the expression of MptD in *M. smegmatis* transformants and on the surface of *M. avium* subsp. *paratuberculosis*. This finding supports the hypothesis that this protein might form a selective pore associated with the outer membrane-like layer of the mycobacterial cell envelope. Furthermore, we developed and used a cell capture PCR technique that employs an fMptD-derived peptide with specific binding capacity for MptD to capture and identify *M. avium* subsp. *paratuberculosis* in raw milk from infected cattle. This demonstrated that the MptD protein is exposed on the surface of *M. avium* subsp. *paratuberculosis* during infection and is therefore a potential target for *M. avium* subsp. *paratuberculosis* immunization or treatment.

These results together with the predicted functions of other genes in the 38-kb region strongly suggest its association with *M. avium* subsp. *paratuberculosis* virulence and that the 38-kb locus should be considered the first pathogenicity island identified in *M. avium* subsp. *paratuberculosis.* The localization of an ABC transporter operon on a putative pathogenicity island has been previously described for *Salmonella enterica* serovar Typhimurium (48), and an ABC transporter also involved in iron uptake has been identified on a pathogenicity island of *Streptococcus pneumoniae* (7). Furthermore, the ABC transporter system of *Y. pestis*, YbtPQ, which also is required for iron uptake and has a significant degree of similarity to the *mpt* operon products of *M. avium* subsp. *paratuberculosis*, is located within a large unstable region of the *Y. pestis* chromosome (18).

Future studies are needed to determine the precise function of the *M. avium* subsp. *paratuberculosis*-specific *fep*, *mpt*, and *sid* operons. The use of specific phage-displayed peptides might be of considerable value in this field by overcoming the problems associated with the extremely slow growth of this organism and the lack of a proven targeted mutagenesis system for *M. avium* subsp. *paratuberculosis*.

The induction of protective immunity against systemic *S. pneumoniae* infection in mice when they are vaccinated with components of iron uptake ABC transporters (8) and the sustained reduction of challenged *M. tuberculosis* growth when mice are vaccinated with a phosphate ABC transporter (46) suggest that the MptD protein may be a suitable component in an *M. avium* subsp. *paratuberculosis* vaccine design. The recent development of a beige/scid mouse model able to demonstrate

intestinal pathophysiologic changes upon *M. avium* subsp. *paratuberculosis* infection (33) may support such studies.

ACKNOWLEDGMENTS

This work has been supported by the Deutsche Forschungsgemeinschaft, Bonn, Germany (Sonderforschungsbereich 280 Gastrointestinale Barriere), and by EU grant QLK 2-CT-2001-01420. Additional support has been provided by the Scottish Executive Rural Affairs Department (SERAD), Scotland, United Kingdom, and the Deutscher Akademischer Austauschdienst, Bonn, Germany. Research in the laboratory of Vivek Kapur is supported by grants from the U.S. Department of Agriculture's National Research Initiative and Agriculture Research Service, the National Institutes of Health, and the Minnesota Agriculture Experiment Station's Rapid Agricultural Response Fund. Research in the laboratory of Tim J. Bull is supported by a grant from Action Medical Research.

REFERENCES

1. **Baichoo, N., and J. D. Helmann.** 2002. Recognition of DNA by Fur: a reinterpretation of the Fur box consensus sequence. J. Bacteriol. **184:**5826–5832.
2. **Barsom, E. K., and G. F. Hatfull.** 1997. A putative ABC-transport operon of *Mycobacterium smegmatis.* Gene **185:**127–132.
3. **Bearden, S. W., J. D. Fetherston, and R. D. Perry.** 1997. Genetic organization of the yersiniabactin biosynthetic region and construction of avirulent mutants in *Yersinia pestis.* Infect. Immun. **65:**1659–1668.
4. **Bentley, S. D., K. F. Chater, A. M. Cerdeno-Tarraga, G. L. Challis, N. R. Thomson, K. D. James, D. E. Harris, M. A. Quail, H. Kieser, D. Harper, A. Bateman, S. Brown, G. Chandra, C. W. Chen, M. Collins, A. Cronin, A. Fraser, A. Goble, J. Hidalgo, T. Hornsby, S. Howarth, C. H. Huang, T. Kieser, L. Larke, L. Murphy, K. Oliver, S. O'Neil, E. Rabbinowitsch, M. A. Rajandream, K. Rutherford, S. Rutter, K. Seeger, D. Saunders, S. Sharp, R. Squares, S. Squares, K. Taylor, T. Warren, A. Wietzorrek, J. Woodward, B. G. Barrell, J. Parkhill, and D. A. Hopwood.** 2002. Complete genome sequence of the model actinomycete *Streptomyces coelicolor* A3(2). Nature **417:**141–147.
5. **Bianchet, M. A., Y. H. Ko, L. M. Amzel, and P. L. Pedersen.** 1997. Modeling of nucleotide binding domains of ABC transporter proteins based on a F-1-ATPase/recA topology: structural model of the nucleotide binding domains of the cystic fibrosis transmembrane conductance regulator (CFTR). J. Bioenerg. Biomembr. **29:**503–524.
6. **Bose, M., A. Chander, and R. H. Das.** 1993. A rapid and gentle method for the isolation of genomic DNA from mycobacteria. Nucleic Acids Res. **21:**2529–2530.
7. **Brown, J. S., S. M. Gilliland, and D. W. Holden.** 2001. A *Streptococcus pneumoniae* pathogenicity island encoding an ABC transporter involved in iron uptake and virulence. Mol. Microbiol. **40:**572–585.
8. **Brown, J. S., A. D. Ogunniyi, M. C. Woodrow, D. W. Holden, and J. C. Paton.** 2001. Immunization with components of two iron uptake ABC transporters protects mice against systemic *Streptococcus pneumoniae* infection. Infect. Immun. **69:**6702–6706.
9. **Burlein, J. E., C. K. Stover, S. Offutt, and M. S. Hanson.** 1994. Expression of foreign genes in mycobacteria, p. 239–252. *In* B. R. Bloom (ed.), Tuberculosis: pathogenesis, protection, and control. ASM Press, Washington, D.C.
10. **Cameron, R. M., K. Stevenson, N. F. Inglis, J. Klausen, and J. M. Sharp.** 1994. Identification and characterization of a putative serine protease expressed in vivo by *Mycobacterium avium subsp. paratuberculosis.* Microbiology **140:**1977–1982.
11. **Carniel, E.** 2001. The *Yersinia* high-pathogenicity island: an iron-uptake island. Microbes Infect. **3:**561–569.
12. **Chiodini, R. J.** 1989. Crohn's disease and the mycobacterioses: a review and comparison of two disease entities. Clin. Microbiol. Rev. **2:**90–117.
13. **Chiodini, R. J., H. J. Van Kruiningen, and R. S. Merkal.** 1984. Ruminant paratuberculosis (Johne's disease): the current status and future prospects. Cornell Vet. **74:**218–262.
14. **Cole, S. T., R. Brosch, J. Parkhill, T. Garnier, C. Churcher, D. Harris, S. V. Gordon, K. Eiglmeier, S. Gas, C. E. Barry, F. Tekaia, K. Badcock, D. Basham, D. Brown, T. Chillingworth, R. Connor, R. Davies, K. Devlin, T. Feltwell, S. Gentles, N. Hamlin, S. Holroyd, T. Hornby, K. Jagels, A. Krogh, J. McLean, S. Moule, L. Murphy, K. Oliver, J. Osborne, M. A. Quail, M. A. Rajandream, J. Rogers, S. Rutter, K. Seeger, J. Skelton, R. Squares, S. Squares, J. E. Sulston, K. Taylor, S. Whitehead, and B. G. Barrell.** 1998. Deciphering the biology of *Mycobacterium tuberculosis* from the complete genome sequence. Nature **396:**190–198.
15. **Drapier, J. C., H. Hirling, J. Wietzerbin, P. Kaldy, and L. C. Kuhn.** 1993. Biosynthesis of nitric oxide activates iron regulatory factor in macrophages. EMBO J. **12:**3643–3649.
16. **El Zaatari, F. A., S. A. Naser, and D. Y. Graham.** 1997. Characterization of a specific *Mycobacterium paratuberculosis* recombinant clone expressing 35,000-molecular-weight antigen and reactivity with sera from animals with clinical and subclinical Johne's disease. J. Clin. Microbiol. **35:**1794–1799.
17. **Fath, M. J., and R. Kolter.** 1993. ABC transporters: bacterial exporters. Microbiol. Rev. **57:**995–1017.
18. **Fetherston, J. D., V. J. Bertolino, and R. D. Perry.** 1999. YbtP and YbtQ: two ABC transporters required for iron uptake in *Yersinia pestis.* Mol. Microbiol. **32:**289–299.
19. **Gerlach, G. F., C. Anderson, A. A. Potter, S. Klashinsky, and P. J. Willson.** 1992. Cloning and expression of a transferrin-binding protein from *Actinobacillus pleuropneumoniae.* Infect. Immun. **60:**892–898.
20. **Hansen-Wester, I., and M. Hensel.** 2001. Salmonella pathogenicity islands encoding type III secretion systems. Microb. Infect. **3:**549–559.
21. **Harris, N. B., and R. G. Barletta.** 2001. *Mycobacterium avium* subsp. *paratuberculosis* in veterinary medicine. Clin. Microbiol. Rev. **14:**489–512.
22. **Hermon-Taylor, J., T. J. Bull, J. M. Sheridan, J. Cheng, M. L. Stellakis, and N. Sumar.** 2000. Causation of Crohn's disease by *Mycobacterium avium* subspecies *paratuberculosis.* Can. J. Gastroenterol. **14:**521–539.
23. **Hernandez, P. M., N. G. Fomukong, T. Hellyer, I. N. Brown, and J. W. Dale.** 1994. Characterization of IS1110, a highly mobile genetic element from *Mycobacterium avium.* Mol. Microbiol. **12:**717–724.
24. **Higgins, C. F.** 1992. ABC transporters: from microorganisms to man. Annu. Rev. Cell Biol. **8:**67–113.
25. **Homuth, M., P. Valentin-Weigand, M. Rohde, and G. F. Gerlach.** 1998. Identification and characterization of a novel extracellular ferric reductase from *Mycobacterium paratuberculosis.* Infect. Immun. **66:**710–716.
26. **Hulten, K., H. M. El Zimaity, T. J. Karttunen, A. Almashhrawi, M. R. Schwartz, D. Y. Graham, and F. A. El Zaatari.** 2001. Detection of *Mycobacterium avium* subspecies *paratuberculosis* in Crohn's diseased tissues by in situ hybridization. Am. J. Gastroenterol. **96:**1529–1535.
27. **Kertesz, M. A.** 2000. Riding the sulfur cycle—metabolism of sulfonates and sulfate esters in gram-negative bacteria. FEMS Microbiol. Rev. **24:**135–175.
28. **Kreeger, J. M.** 1991. Ruminant paratuberculosis—a century of progress and frustration. J. Vet. Diagn. Invest. **3:**373–382.
29. **Lisitsyn, N., N. Lisitsyn, and M. Wigler.** 1993. Cloning the differences between two complex genomes. Science **259:**946–951.
30. **Lisitsyn, N. A.** 1995. Representational difference analysis: finding the differences between genomes. Trends Genet. **11:**303–307.
31. **McClure, H. M., R. J. Chiodini, D. C. Anderson, R. B. Swenson, W. R. Thayer, and J. A. Coutu.** 1987. *Mycobacterium paratuberculosis* infection in a colony of stumptail macaques (*Macaca arctoides*). J. Infect. Dis. **155:**1011–1019.
32. **Mutharia, L. M., W. Moreno, and M. Raymond.** 1997. Analysis of culture filtrate and cell wall-associated antigens of *Mycobacterium paratuberculosis* with monoclonal antibodies. Infect. Immun. **65:**387–394.
33. **Mutwiri, G. K., U. Kosecka, M. Benjamin, S. Rosendal, M. Perdue, and D. G. Butler.** 2001. *Mycobacterium avium* subspecies *paratuberculosis* triggers intestinal pathophysiologic changes in beige/scid mice. Comp. Med. **51:**538–544.
34. **Nielsen, K., and P. Ahrens.** 2002. Putative in vitro expressed gene fragments unique to *Mycobacterium avium* subspecies *paratuberculosis.* FEMS Microbiol. Lett. **214:**199–203.
35. **Raleigh, F., A. K. Lech, and R. Brent.** 1989. Selected topics from classical bacterial genetics, p. 1.4.1–1.4.14. *In* F. M. Ausubel et al. (ed.), Current protocols in molecular biology. Wiley Interscience, New York, N.Y.
36. **Rodriguez, G. M., and I. Smith.** 2003. Mechanisms of iron regulation in mycobacteria: role in physiology and virulence. Mol. Microbiol. **47:**1485–1494.
37. **Sambrook, J., E. F. Fritsch, and T. Maniatis.** 1989. Molecular cloning: a laboratory manual, 2nd ed. Cold Spring Harbor Laboratory, Cold Spring Harbor, N.Y.
38. **Sander, P., and E. C. Boettger.** 1998. Gene replacement in *Mycobacterium smegmatis* using a dominant negative selectable marker, p. 207–216. *In* T. Parish and N. G. Stoker (ed.), Mycobacteria protocols. Humana Press Inc., Totowa, N.J.
39. **Schell, M. A., M. Karmirantzou, B. Snel, D. Vilanova, B. Berger, G. Pessi, M. C. Zwahlen, F. Desiere, P. Bork, M. Delley, R. D. Pridmore, and F. Arigoni.** 2002. The genome sequence of *Bifidobacterium longum* reflects its adaptation to the human gastrointestinal tract. Proc. Natl. Acad. Sci. USA **99:**14422–14427.
40. **Schubert, S., D. Fischer, and J. Heesemann.** 1999. Ferric enterochelin transport in *Yersinia enterocolitica*: molecular and evolutionary aspects. J. Bacteriol. **181:**6387–6395.
41. **Secott, T. E., T. L. Lin, and C. C. Wu.** 2001. Fibronectin attachment protein homologue mediates fibronectin binding by *Mycobacterium avium* subsp. *paratuberculosis.* Infect. Immun. **69:**2075–2082.
42. **Snapper, S. B., R. E. Melton, S. Mustafa, T. Kieser, and W. R. Jacobs, Jr.** 1990. Isolation and characterization of efficient plasmid transformation mutants of *Mycobacterium smegmatis.* Mol. Microbiol. **4:**1911–1919.
43. **Snyder, L., and W. Champness.** 1997. Molecular genetics of bacteria, p. 55. ASM Press, Washington, D.C.
44. **Stratmann, J., B. Strommenger, K. Stevenson, and G. F. Gerlach.** 2002. Development of a peptide-mediated capture PCR for detection of *Mycobacterium avium* subsp. *paratuberculosis* in milk. J. Clin. Microbiol. **40:**4244–4250.

45. **Strommenger, B., K. Stevenson, and G. F. Gerlach.** 2001. Isolation and diagnostic potential of IS*Mav2*, a novel insertion sequence-like element from *Mycobacterium avium ssp. paratuberculosis.* FEMS Microbiol. Lett. **196:**31–37.
46. **Tanghe, A., P. Lefevre, O. Denis, S. D'Souza, M. Braibant, E. Lozes, M. Singh, D. Montgomery, J. Content, and K. Huygen.** 1999. Immunogenicity and protective efficacy of tuberculosis DNA vaccines encoding putative phosphate transport receptors. J. Immunol. **162:**1113–1119.
47. **Tizard, M., T. Bull, D. Millar, T. Doran, H. Martin, N. Sumar, J. Ford, and J. Hermon-Taylor.** 1998. A low G+C content genetic island in *Mycobacterium avium* subsp. *paratuberculosis* and *M. avium* subsp. *silvaticum* with homologous genes in *Mycobacterium tuberculosis.* Microbiology **144:**3413–3423.
48. **Zhou, D., W. D. Hardt, and J. E. Galan.** 1999. *Salmonella typhimurium* encodes a putative iron transport system within the centisome 63 pathogenicity island. Infect. Immun. **67:**1974–1981.

Editor: B. B. Finlay